Author/s:
Reid, KJ;Rosier, SM;Harrington, LJ;King, AD;Lane, TP

Title:
Extreme rainfall in New Zealand and its association with Atmospheric Rivers

Date:
2021-04-01

Citation:
Reid, K. J., Rosier, S. M., Harrington, L. J., King, A. D. & Lane, T. P. (2021). Extreme rainfall in New Zealand and its association with Atmospheric Rivers. Environmental Research Letters, 16 (4), https://doi.org/10.1088/1748-9326/abeae0.

Persistent Link:
https://hdl.handle.net/11343/274393

ENVIRONMENTAL RESEARCH
LETTERS

LETTER • OPEN ACCESS

Extreme rainfall in New Zealand and its association with Atmospheric Rivers

To cite this article: Kimberley J Reid *et al* 2021 *Environ. Res. Lett.* **16** 044012

ENVIRONMENTAL RESEARCH
LETTERS

OPEN ACCESS

RECEIVED
16 September 2020

REVISED
19 February 2021

ACCEPTED FOR PUBLICATION
1 March 2021

PUBLISHED
12 March 2021

LETTER

Extreme rainfall in New Zealand and its association with Atmospheric Rivers

Kimberley J Reid[1,*], Suzanne M Rosier[2], Luke J Harrington[3,4], Andrew D King[1] and Todd P Lane[1]

[1] The School of Earth Sciences and ARC Centre of Excellence for Climate Extremes, The University of Melbourne, Parkville, Victoria, Australia
[2] The National Institute of Water and Atmospheric Research, Wellington, New Zealand
[3] Environmental Change Institute, University of Oxford, Oxford, United Kingdom
[4] New Zealand Climate Change Research Institute, School of Geography, Environment and Earth Sciences, Victoria University of Wellington, Wellington, New Zealand
[*] Author to whom any correspondence should be addressed.

E-mail: kimberleyr@student.unimelb.edu.au

Keywords: rainfall extremes, atmospheric rivers, New Zealand, flooding

Supplementary material for this article is available online

Abstract

Atmospheric rivers (ARs) are narrow and elongated regions of enhanced horizontal water vapour transport. Considerable research on understanding Northern Hemisphere ARs and their relationship with extreme precipitation has shown that ARs have a strong association with heavy rainfall and flooding. While there has been very little work on ARs in the Southern Hemisphere, global climatologies suggest that ARs are equally as common in both hemispheres. New Zealand in particular is located in a region of high AR frequency. This study aims to test the hypothesis that ARs play a significant role in heavy precipitation and flooding events in New Zealand. We used a recently developed AR identification method and daily station data across New Zealand to test for the concurrence of ARs and extreme rainfall. We found that, at each of the eleven stations analysed, at least seven to all ten of the top ten heaviest precipitation days between 1980 and 2018 were associated with AR conditions. Nine of the ten most damaging floods in New Zealand between 2007 and 2017 occurred during AR events. These results have important implications for understanding extreme rainfall in New Zealand, and ultimately for predicting some of the most hazardous events in the region. This work also highlights that more research on ARs in New Zealand is needed.

1. Introduction

New Zealand is located between 34 and 47° S, with a mountain range extending the length of the North and South Islands in the path of the prevailing mid-latitude westerlies. Broadly speaking, there are four main rainfall regimes: uplift and rainfall from fronts and cyclones within the westerlies; orographically enhanced rainfall; free convection and thunderstorm development triggered by summer heating; and subtropical synoptic systems from the north (Tait and Fitzharris 1998). This research focuses on the hypothesis that atmospheric rivers (ARs) play an important role in New Zealand's rainfall and its extremes.

Flooding from heavy rainfall is one of the many hazards faced by New Zealanders. Ericksen (1986) estimated that the nine most serious floods in New Zealand between 1968 and 1984 cost $NZ 353 million collectively (adjusted for inflation to 2020 Q3 using the New Zealand Reserve Bank inflation calculator www.rbnz.govt.nz/monetary-policy/inflation-calculator). More recently, the Insurance Council of New Zealand estimated that the 12 most expensive floods between 2007 and 2017 cost $NZ 472 million (ICNZ; Frame *et al* 2020).

ARs are long, narrow regions of intense water vapour transport (Newell *et al* 1992). The Guan and Waliser (2015) global climatology of ARs found a high frequency of landfalling ARs along coastal regions of Australia and New Zealand (NZ). Moreover, they found that AR frequency peaked at approximately 41° S, coinciding with the mean latitude of NZ. Thus, NZ appears to be a location of high AR activity.

Ralph *et al* (2006) was one of the first studies to empirically link ARs with extreme weather. They analysed seven floods that occurred on the Russian River, California, between October 1997 and February 2006 using radar and satellite observations of wind and integrated water vapour respectively. It was found that all seven floods were associated with heavy rainfall caused by orographic precipitation associated with ARs. Nayak and Villarini (2017) analysed Central USA hydrological impacts of ARs using station records of 60–80 years. From these long-term records they showed that annually about 40% of daily extreme precipitation events (defined as above the 99th percentile) were associated with ARs and up to 70%–90% of extreme rainfall events in winter were associated with ARs.

While North American-focused analyses of ARs and their impacts dominate the AR literature, there have been a number of studies demonstrating that ARs have considerable impacts elsewhere. Lavers *et al* (2011) described ARs as critical in explaining extreme winter flooding in the UK and demonstrated that ARs were responsible for the ten largest winter floods in Britain since the 1970s. Additionally, ARs have been associated with extreme precipitation and flooding leading to considerable socio-economic impacts over the Iberian Peninsula (Ramos *et al* 2015, Eiras-Barca *et al* 2018). In the Southern Hemisphere, about half of the extreme daily rainfall in Central-Southern Chile is associated with ARs (Valenzuela and Garreaud 2019), while around 70% of extreme winter rainfall was associated with ARs in South Africa (Blamey *et al* 2018). Paltan *et al* (2017) modelled the global relationship between AR rainfall and hydrological parameters and found that more than 50% of mean annual runoff on the west coast and North Island of New Zealand was associated with AR precipitation. Studies from around the world have shown that ARs can have significant impacts like extreme rainfall and associated flooding due to the very large volume of moisture the systems can transport. However, most of the literature has focused on the Northern Hemisphere, with Southern Hemisphere ARs relatively under-studied.

Regarding New Zealand, Kingston *et al* (2016) analysed the role of ARs in contributing to floods via enhanced snowmelt on the NZ Southern Alps due to both rain on snow causing melting and the advection of warmer air masses from the northwest. They found that all eight major winter floods on the Waitaki River (South Island) between 1979 and 2012 were associated with ARs. A separate study (Little *et al* 2019) found ARs to influence both extreme ablation and snowfall on the NZ Southern Alps, while Cullen *et al* (2019) and Porhemmat *et al* (2020) showed a link between ARs and the largest snowfall events in the same region. Some case studies of extreme rainfall events in New Zealand have indicated an influence of ARs (Dean *et al* 2013, Rosier *et al* 2015). However, despite previous indications that ARs occur frequently over NZ and can cause extreme rainfall and flooding, especially where the prevailing westerlies meet the mountain ranges, there is currently no study explicitly documenting the role of ARs in New Zealand extreme rainfall and flooding comprehensively for the whole country.

In this article, we aim to build on this previous work by analysing the most extreme rainfall days (since 1980, or thereafter) at each of 11 stations throughout NZ, and also the most damaging recent flooding events (as measured by insured losses). In both cases, we determine the extent to which ARs are associated with extreme rainfall and flooding in New Zealand.

2. Data and methods

2.1. Heavy rainfall and flooding data

We used daily rainfall data from the New Zealand National Climate Database at 11 stations across New Zealand: Auckland, Christchurch, Dunedin, Gisborne, Greymouth, Hamilton, Milford Sound, Nelson, New Plymouth, Tauranga and Wellington (figure 1).

Almost all were automatic weather stations at which daily rainfall accumulations were measured using standard tipping bucket rain gauges with a resolution of 0.2 mm; at one station (Milford Sound) the record used was a manual rain gauge reading (at 9 am daily) at a resolution of 0.1 mm. The tipping bucket technique tends to under-record rainfall amounts compared to the manual process; however, the use of data from both techniques was not deemed to be a significant issue for the purposes of this study, namely identifying the dates of the most extreme rainfall amounts. At each location, the station was chosen to maximise the length and completeness of the record, whilst also stipulating that the record finish in the present.

At each station, we ranked daily rainfall amounts to find the days of the top ten daily rainfalls. In order to have ten (temporally) independent days to examine, we stipulated that if any of the top ten days were within one week of each other, we only retained the single day with the highest rainfall amount. We used rainfall events between 1980 and 2018 to coincide with the available AR data (see section 2.2). We also analysed the top ten costliest floods between 2007 and 2017 as determined by insured losses from the Insurance Council of New Zealand (ICNZ; Frame *et al* 2020); we did so in order to investigate socio-economic impacts of extreme rainfall, as well as the rainfall itself. By investigating the relationship between ARs and costly impacts we hope to encourage future research aimed at forecasting ARs at daily to seasonal scales, together with its implications for emergency management (Lavers *et al* 2014). It is worth noting that the costs of these flooding events have likely been underestimated given that the metric

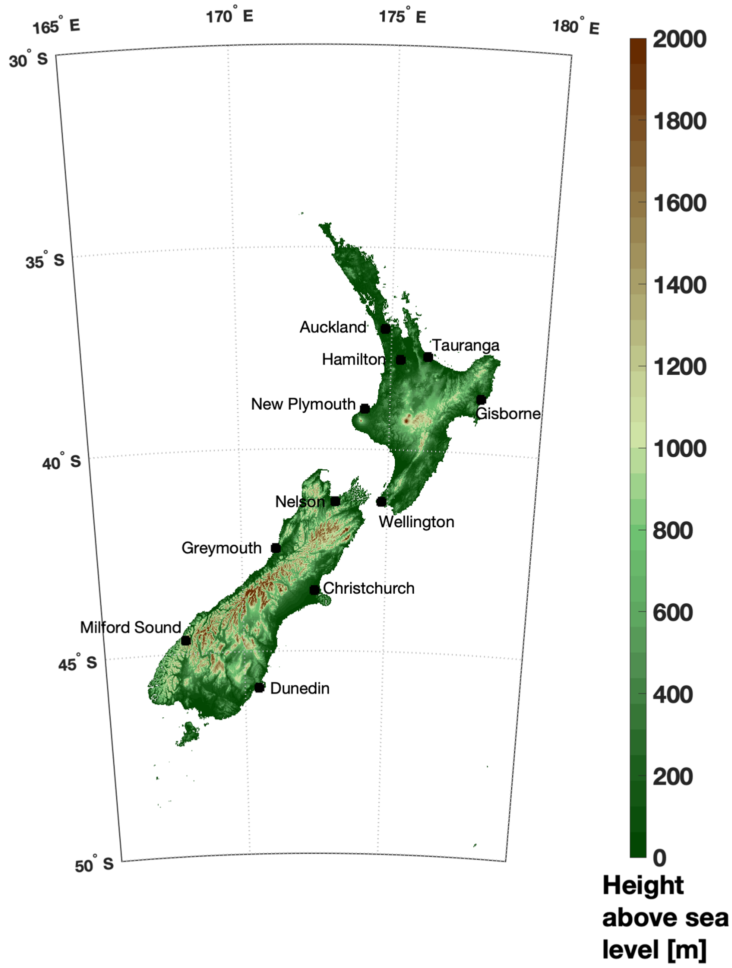

Figure 1. Map of New Zealand topography and stations used in this study (elevation data courtesy of NASA WorldWind and data from the Shuttle Radar Topography Mission).

of insured losses does not include publicly owned assets and damage to uninsured property (Frame *et al* 2020).

2.2. AR identification

We used the Reid *et al* (2020) AR identification algorithm where the boundary of an AR is defined as integrated water vapour transport (IVT) greater than or equal to 500 kg m^{-1} s^{-1}. We chose to use an identification method with an absolute IVT threshold as recommended, by Rutz *et al* (2019), for midlatitude studies. Additionally, we use a restrictive threshold of 500 kg m^{-1} s^{-1} because of the risk identified in Reid *et al* (2020) that lower-threshold algorithms with some geometric criteria may miss the most intense ARs. IVT was calculated using the three hourly Modern-Era Retrospective analysis for Research and Applications Version 2 reanalysis (MERRA2; Gelaro *et al* 2017) as part of the Atmospheric River Tracking Method Intercomparison Project (ARTMIP; Shields *et al* 2018). The Reid *et al* identification algorithm identifies spatially continuous regions of IVT above the selected threshold and then calculates geometric parameters including: AR centroid location, major and minor axes lengths, orientation angle (relative to line of latitude), and mean and maximum IVT. The algorithm then excludes potential ARs if they do not meet the following criteria: major axis length is greater than 2000 km, length to width ratio is greater than two, and the orientation angle relative to latitude is greater than 10° (to exclude the Inter-Tropical Convergence Zone).

We calculated AR frequency using the Reid *et al* (2020) algorithm for NZ (figure 2). We found a strong seasonal cycle in AR occurrence and the highest frequency in Austral summer (December January February; DJF) over New Zealand. This is distinct from North American and European west coast analyses that have found that ARs are more frequent in the cooler months (Rutz *et al* 2019). However, studies in the Northwest Pacific also found that AR frequency peaked in the warm season. This has been linked to atmosphere-ocean coupling in the tropical Indian and Pacific Oceans, as opposed to the more midlatitude driven ARs that dominate eastern ocean basins (Kamae *et al* 2017, Pan and Lu 2020). A secondary region of high AR frequency is apparent in winter (June July August; JJA) although

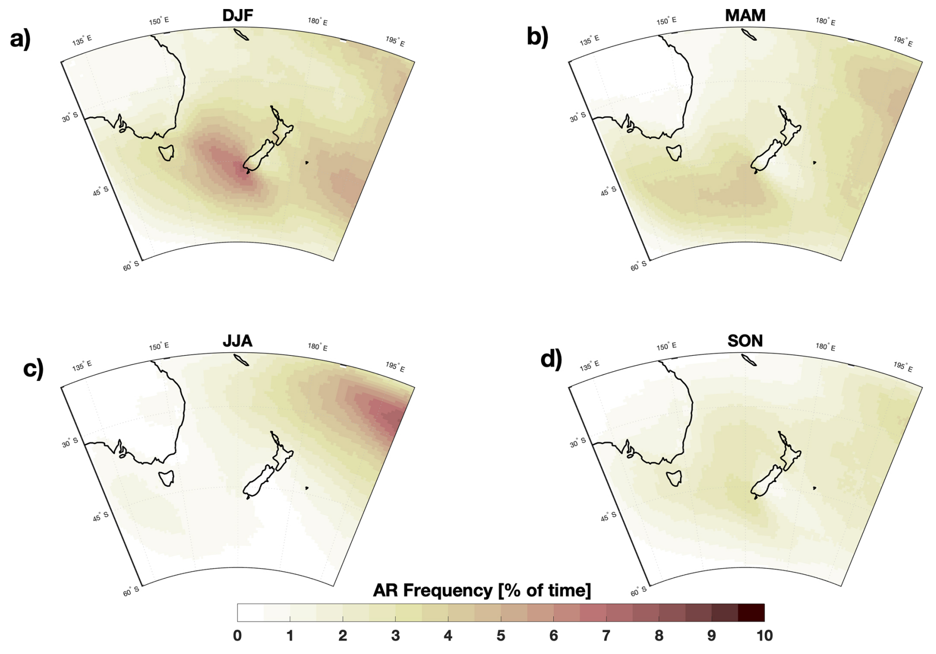

Figure 2. Percentage of times (three hourly intervals) between 1980 and 2018 when an AR is present, by season.

somewhat further from New Zealand land. These ARs occur well to the northeast of the country but are entirely consistent with previous studies (Rosier *et al* 2015 supplementary material (available online at stacks.iop.org/ERL/16/044012/mmedia)), which found ARs in the northeast brought onshore by (north)easterly flow to be an important mechanism in winter extreme rainfall events (see also figure 4). More work is needed to understand the drivers of the AR annual cycle in the Australasian region. Figure 2 shows a distinct AR shadow on the lee side of the New Zealand mountain ranges for all seasons with a stronger signal over and in the lee side of the South Island where the mountains are taller. This phenomenon has also been observed in the Western USA where ARs typically decay after interacting with orography and precipitating out moisture and wind speeds are reduced (Rutz *et al* 2015).

To test whether an AR was associated with an extreme rainfall event, we produced an AR mask (masking where an AR was identified) every 3 h between 1980 and 2018, and in the region 130° E to 200° E longitude and 15° S to 60° S latitude. If an AR was identified over the location in question on the day or day before the heavy rainfall or flooding event, that event was considered to be associated with an AR. Figures 3(a) and (c) demonstrate examples of masked ARs during the rank-one rainfall events at Milford Sound (West coast of the South Island) and Auckland (Northwestern part of the North Island). We further verified each event using satellite imagery (Knapp *et al* 2011), by looking for narrow, large-scale cloudbands, and official reports by interrogating the National Institute of Water and Atmospheric Research (NIWA) historic weather events catalogue (https://hwe.niwa.co.nz/).

Table 1. Number of the top ten rainfall events that were associated with an AR for each station.

Station	Number of top ten rainfall events associated with an AR
Auckland	9
Christchurch	8
Dunedin	9
Gisborne	8
Greymouth	9
Hamilton	8
Milford Sound	9
Nelson	9
New Plymouth	8
Tauranga	7
Wellington	10

3. Results and discussion

Our results indicate a strong association between damaging New Zealand precipitation events and ARs. Table 1 lists how many of the top ten precipitation days at each station coincided with an AR event at that location. A more detailed list of each event is available in the supplementary material. About 60% of extreme rainfall events (regardless of an AR being present) occurred between January and April, while August and September combined account for 3.5% of events. Six of the events were spatially concurrent at two stations (e.g. Auckland and Tauranga; Christchurch and Wellington; Greymouth and Nelson) and one event occurred at three stations (Auckland, Hamilton and

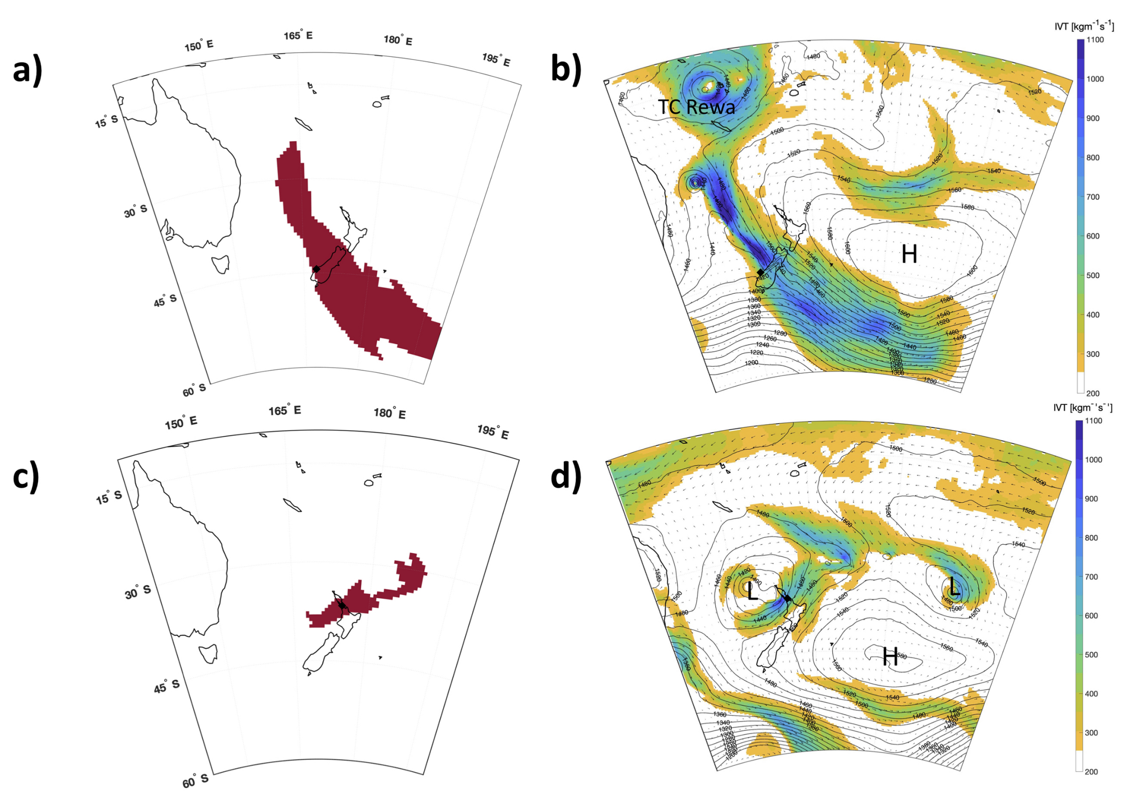

Figure 3. (a) Mask showing identified AR during rank-one Milford Sound rainfall event (1800UTC, 21 January 1994), (b) coloured contours are IVT during rank-one Milford Sound rainfall event and black contours are geopotential height at 850 hPa level, (c) and (d) are the same as (a) and (b) but for the rank-one Auckland rainfall event (0000UTC, 16 February 1985). Black diamonds indicate locations in question.

Tauranga on the 5th of April, 2017). This is not surprising given these stations' geographical proximity.

We found that, depending on the station, between seven and all ten of the top ten New Zealand rainfall events were associated with ARs. All ten heaviest rainfall events were associated with ARs at Wellington. Interestingly, most of the top ten extreme rainfall days at Dunedin and Christchurch (East Coast South Island, figure 1) were still associated with ARs (nine and eight respectively) despite being located in the aforementioned AR shadow. Both rank-one rain events for Dunedin and Christchurch were associated with ARs which had orientation angles between 70° to 80°. In comparison the rank-one Milford Sound event shown in figures 3(a) and (b) had an AR orientation angle of approximately 40°. In other words, the most extreme rainfall days on the East coast were associated with more meridional AR events. Despite the AR shadow, east coast cities are still vulnerable to strong AR events.

Figure 3 illustrates the AR and IVT field for two case studies: the rank-one rainfall days at the Auckland and Milford Sound stations. Figure 3(b) shows the IVT field for the heaviest rain day at Milford Sound (1800UTC, 21 January 1994). The AR is linked with tropical moisture from tropical cyclone (TC) Rewa, which is situated to the northwest of Vanuatu. This intense moisture transport combined with the orographic forcing at Milford Sound led to a record 537.5 mm of rain falling in 24 h. Figure 3(d) shows the IVT field for the rank-one rainfall day at Auckland station (161.8 mm). In contrast to the previous case, the AR and associated moisture came from the northeast. An extratropical cyclone to the northwest of the North Island and anticyclone to the east of NZ advected the warm moist air towards Auckland and surrounding regions. This type of blocking pattern was identified by Kidson (2000) in his study of New Zealand weather regimes and was associated with enhanced precipitation in the northeast.

We repeated this analysis for the ten costliest floods between 2007 and 2017 as described by Frame *et al* (2020). We found that nine of the ten floods were associated with an AR event. Table 2 shows the start and end time and location of each AR, together with an indication of its mean and peak intensity (IVT). In some cases, the AR was concurrent with another weather event; for example, in the case of flood rank-two, the AR transported enhanced moisture from the remnants of TC Debbie towards New Zealand. The interaction between TCs and ARs have been observed elsewhere. Cordeira *et al* (2013) analysed two ARs that made landfall in Northern California that had developed in conjunction with TCs in the western North Pacific. Using parcel trajectory analysis, they showed that the landfalling AR parcels

Table 2. Top ten most expensive NZ floods between 2007 and 2017 and associated AR details.

Flood rank	Year	Date	Location	Cost ($m)	AR	Start time	Start centroid (lat, lon)	End time	End centroid (lat, lon)	Mean daily max IVT (kg m s^{-1})	Max daily IVT during event (kg m s^{-1})
1	2007	10–12 July	North North Island	68.65	Yes	12UTC 10 July	(−27 179.4)	00UTC 13 July	(−22.5192.5)	1155	1434
2	2017	3–7 April	North Island	66.4	Yes	12UTC 6 April	(−43.0,188.1)	12UTC 7 April	(−45.0,198.1)	1073	1116
3	2013	19–22 April	Nelson, Bay of Plenty	46.2	No	—	—	—	—	—	—
4	2017	7–12 March	Upper North Island	41.7	Yes	00UTC 6 March	(−30.0,162.5)	15UTC 12 March	(−42.5193.8)	1065	1232
5	2015	18–21 June	Lower North Island	41.5	Yes	00UTC 17 June	(−36.5156.2)	12UTC 22 June	(−39.5194.4)	890	1019
6	2016	23–24 March	West Coast—Nelson	30.2	Yes	06UTC 22 March	(−38.0,168.8)	15UTC 24 March	(−51.0, 189.4)	1424	1596
7	2015	2–4 June	Otago	21.5	Yes	03UTC 1 June	(−30.0,164.4)	21UTC 4 June	(−45.5198.8)	753	930
8	2015	13–15 May	Lower North Island	21.9	Yes	12UTC 12 May	(−42.5181.9)	15UTC 17 May	(−46.0, 198.8)	906	1063
9	2011	29-Jan	Northland—BoP	19.8	Yes	21UTC 26 Jan	(−24.5177.5)	06UTC 29 Jan	(−41.0, 186.9)	1967	2297
10	2014	8–10 July	Northland	18.8	Yes	12UTC 7 July	(−26.5171.3)	21UTC 8 July	(−28.0, 180.0)	1176	1397

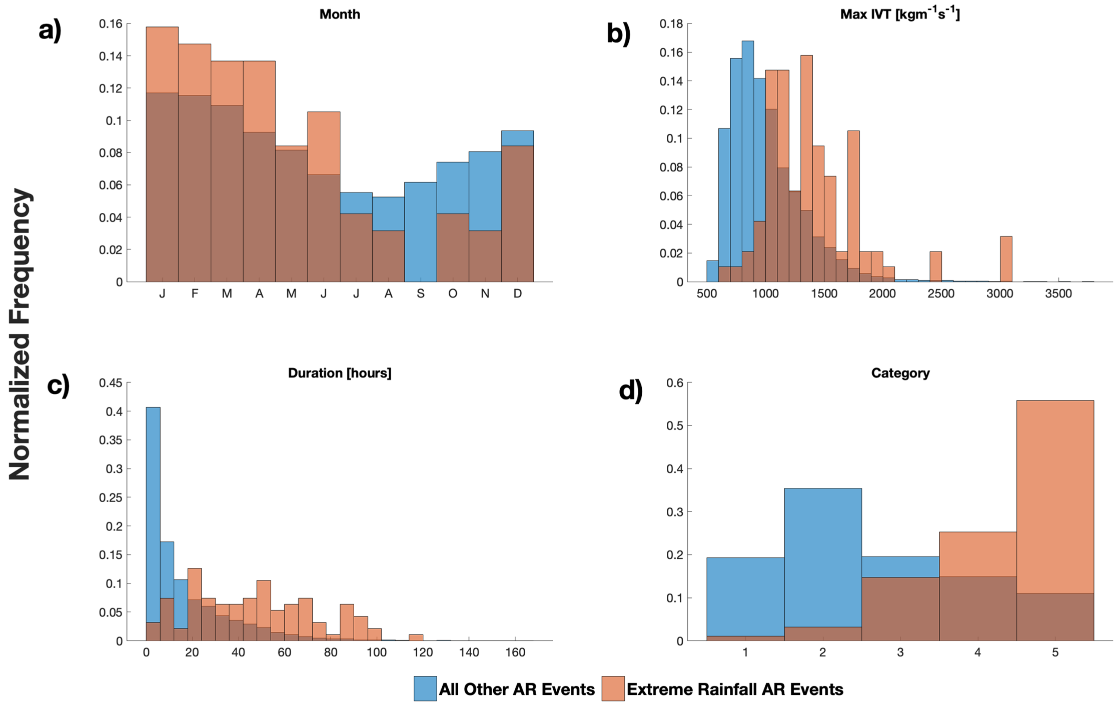

Figure 4. Normalised histograms of (a) month of occurrence, (b) maximum IVT (kg m^{-1} s^{-1}), (c) duration (h), (d) and strength category (Ralph *et al* 2019) for all ARs between 135° and 200° longitude and −15° to −60° latitude, and from 1980 to 2018 (blue), and for the ARs associated with the top ten most extreme rainfall events for each station (brown).

originally underwent deep tropical ascent within the TCs before traversing the North Pacific via the jet stream. The interaction between TCs and ARs in the Tasman Sea is a potential area for future research in understanding extreme rainfall in New Zealand. The one flooding event that did not have an AR associated with it (rank-three) was due to complex extratropical cyclones over the Tasman Sea (see supplementary figure 1 for MSLP chart). The occurrence of an AR does not always lead to extreme rainfall, although as tables 1 and 2 indicate, the most extreme rainfall events are unlikely without an AR.

Figure 4 summarises various different characteristics of the ARs that were associated with the top ten rainfall events and puts them in context of ARs in the region more generally. Brown bars in the histograms represent the ARs associated with the top ten rainfall events, whilst blue bars represent all AR events from 1980 to 2018 in the region 135° E to 200° E, 15° S to 60° S. Figure 4(a) shows the normalised frequency of AR occurrence in each month. Figure 2 showed ARs to be more frequent in Austral summer; however, the annual cycle is seen to be more pronounced for ARs that lead to extreme rainfall. The peak in January to April (figure 4(a)) is likely due to increased moisture availability in the warmer months and, as discussed previously, the interaction with TCs. The difference in the seasonality of ARs associated with the top ten rainfall events (brown), compared with ARs in general (blue), hints at the importance of ARs in extreme rainfall in winter. As noted previously, this is consistent with our previous studies of winter events in which ARs to the northeast, brought onshore by (north)easterly flow, are important. We speculate that this could be the dominant mechanism leading to extreme rainfall in winter; however, further investigation is necessary, and a future study on this would be beneficial. Figure 4(b) summarises the maximum IVT. There is a statistically significant shift in the distribution of maximum IVT for ARs associated with extreme rainfall ($p < 0.05$ using the Kolmogorov–Smirnov test) indicating that the ARs that lead to extreme rainfall are generally stronger than other ARs. However, there is also considerable overlap between the two distributions suggesting that extreme rainfall can occur during a moderate AR event. One such example is the rank-one Auckland case described earlier where the interaction with other synoptic features (extratropical cyclone) and convergence of tropical moisture due to the blocking high to the east of NZ were important factors for causing extreme rainfall from a moderate AR. Figure 4(c) shows the distributions of AR event duration. It is clearly seen that ARs associated with extreme rainfall tend to last longer.

The results of figures 4(b) and (c) are summarised in figure 4(d) using the strength categories developed by Ralph *et al* (2019) that take into account maximum IVT and duration: a category 1 AR would be considered weak and primarily beneficial, while a category 5 AR would be considered strong and primarily hazardous. Category 5 ARs have

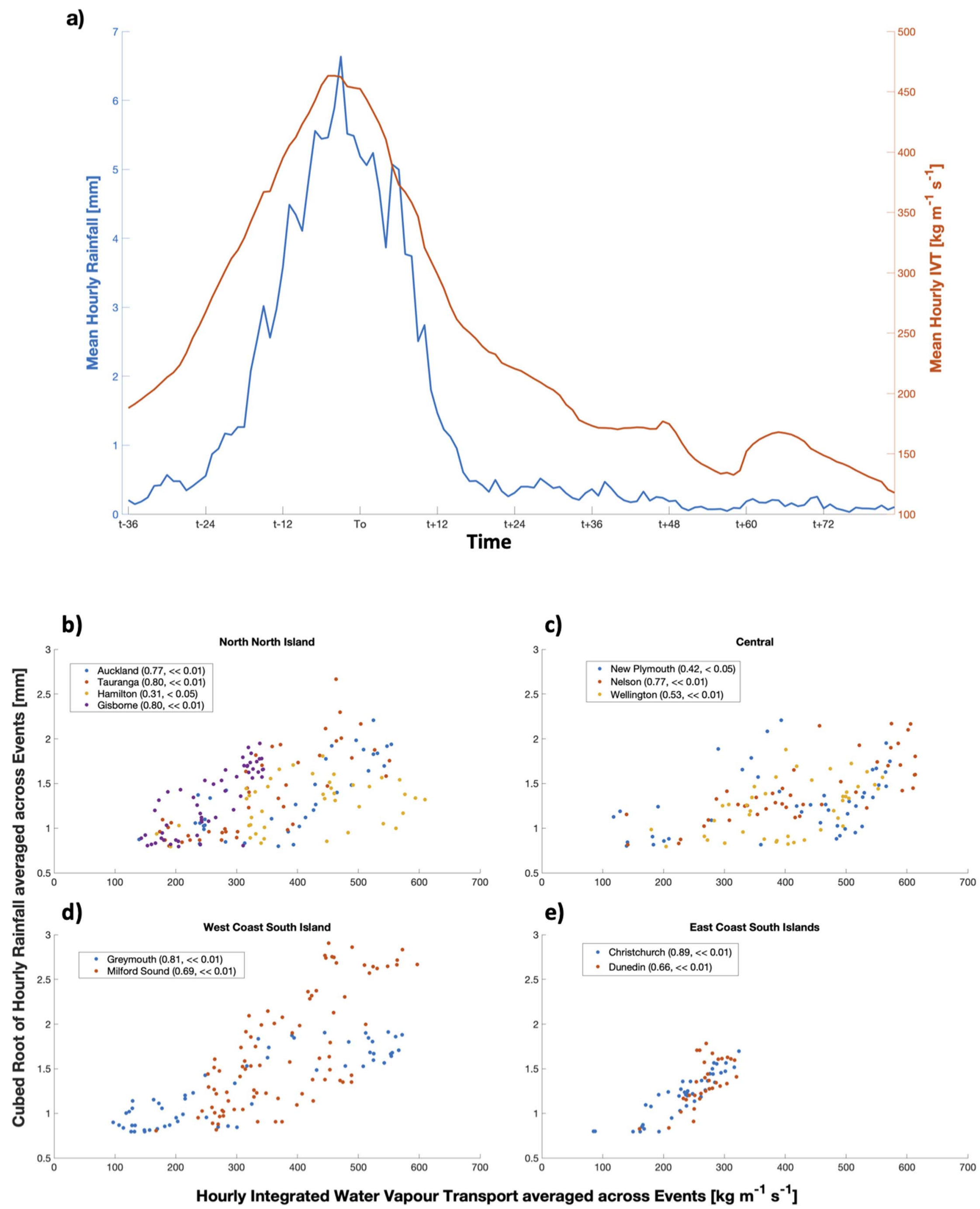

Figure 5. (a) Composite of cubed-root of hourly rainfall (mm) and IVT (kg m^{-1} s^{-1}) for the top ten rainfall events (associated with an AR) for each station. Timeseries is relative to the maximum rainfall day for each event, and (b)–(e) scatterplot of composite hourly IVT versus the cube root of composite hourly rainfall for each station and grouped by region. Rainfall is from station data and IVT is from the ERA5 reanalysis for the 0.25° × 0.25° grid cell that included the station where the rainfall was recorded. Numbers in brackets next to station name indicates the Spearman rank correlation coefficient (left) and *p*-value (right).

a maximum IVT value of 1250 kg m^{-1} s^{-1} and last for at least 24 h, or they may have a max IVT value between 1000 and 1250 kg m^{-1} s^{-1} but last for longer than 48 h. Given we use an AR threshold of 500 kg m^{-1} s^{-1} in our identification method, the range for a category 1 will be smaller than other studies. In this study, a category 1 AR has a maximum IVT value between 500 and 750 kg m^{-1} s^{-1} and duration less than 24 h (table 2 of Ralph *et al* 2019). These AR categories are starting to be used in experimental forecasts (DeFlorio *et al* 2019) and, thus, are worth examining here for relative impacts on rainfall extremes. Figure 4(d) shows a strong shift towards higher category ARs being associated with extreme rainfall; while category 5 is the least common category for all AR events between 1980 and 2018, it is the most common category for AR events that are associated with extreme rainfall. A similar study of flood damage from ARs in the USA found that only a small number of extreme ARs were responsible for a large proportion of flood damages, and that flood damages increased exponentially with AR category (Corringham *et al* 2019).

Since the maximum IVT value of the AR associated with rainfall does not necessarily occur at the same time and location as the rainfall at the station, we also analysed the IVT at the grid cell over each station. We used 5 d of hourly rainfall and IVT from the high resolution ERA5 reanalysis centred on the highest rainfall day (Hersbach *et al* 2019). Given the times used were relative to the event maximum, we could create a composite timeseries of all of the top-ten events for each station (figure 5(a)). We found that, on average, the maximum hourly IVT and maximum hourly rainfall at a station occurred simultaneously. There were individual events where the maximum IVT occurred after the maximum rainfall (see supplementary figure 2) including the rank-one rainfall event at Auckland. We suspect this is due to the northerly AR acting as a moisture feeder to the extratropical cyclone that was situated over Auckland and associated with the intense hourly rainfall (figure 3(d); Dacre *et al* 2019). The centroid of the AR passed over Auckland station after the cyclone had moved away, hence the maximum IVT occurred after the maximum rainfall. The interaction between ARs and other synoptic systems is a potential avenue for further research. We show plots of rainfall and IVT for each of the top ten rainfall events at each station in supplementary figure 2.

To better understand the relationship between IVT and rainfall, we also show scatter plots (figures 5(b)–(e)) of hourly IVT versus the cube root of hourly rainfall for each station (data are a composites of all events as in figure 5(a), and only hourly rainfall values above 0.5 mm are included). The purpose of taking the cube root of rainfall is to normalise the distribution and make it easier to compare stations with different rainfall climatologies (Stidd 1953). We grouped the stations into four regions: North North Island, central, West and East coasts of the South Island. The coastal regions (figures 5(d) and (e)) have strong rainfall-IVT relationships, although the magnitude of IVT and rainfall is lowest on the East Coast. Excluding Hamilton, the North North Island stations have a very strong relationship between IVT and rainfall, but Hamilton itself has the weakest relationship indicating that geographic region does not necessarily dictate the IVT–rainfall relationship. This suggests there may be some local factors that impact the efficiency of ARs, which is a potential avenue for future research. The results in figure 5 increase confidence that the extreme rainfall events analysed in this study are associated with the passage of the AR over their location; however future studies would be beneficial for confirming this relationship.

4. Conclusion

Our analyses indicate that ARs are an important factor in producing damaging rainfall in New Zealand. Nine out of ten of the most expensive floods between 2007 and 2017 occurred during an AR event, and seven to all of the ten heaviest precipitation days at eleven stations analysed here were also associated with ARs. These results complement existing international analyses on AR impacts which have found that ARs are vital for extreme hydrological events (e.g. Ralph *et al* 2006, Lavers *et al* 2011). Despite the clear relationship between ARs and extreme rainfall events in New Zealand that we have demonstrated here, there has been relatively little previous published research of the processes, forecasting and projection of these damaging events. Further work should focus on better understanding the mechanisms that cause only some ARs to produce heavy rainfall. Enhanced understanding of ARs and extreme precipitation, and the variability and trends in ARs in the New Zealand region, should eventually improve the ability to predict high-impact events.

Data availability statement

The data that support the findings of this study are openly available at the following URL/DOI: www.earthsystemgrid.org/dataset/ucar.cgd.ccsm4.artmip.tier1.reid500.html.

Acknowledgments

The work of K J Reid was funded by an Australian Government Research Training Program (RTP) Scholarship and the Australian Research Council (ARC; DE180100638), the work of A D King was funded by the ARC (DE180100638), and the work of T P Lane was funded by the ARC Centre of Excellence for Climate Extremes (CE170100023). S M Rosier was supported by funds from the New Zealand government via a NIWA Climate, Atmosphere and Hazards SSIF programme. L J Harrington and S M Rosier were supported by the New Zealand MBIE Endeavour Fund *Whakahura* programme. We would like to acknowledge high-performance computing support from Cheyenne (doi:10.5065/D6RX99HX) provided by NCAR's Computational and Information Systems Laboratory, sponsored by the National Science Foundation.

We are very grateful to Errol Lewthwaite, Linda Wang, Seema Singh and Andrew Harper for their help with the station rainfall data from the NIWA National Climate Database.

ORCID iDs

Kimberley J Reid https://orcid.org/0000-0001-5972-6015
Suzanne M Rosier https://orcid.org/0000-0002-0673-5847
Luke J Harrington https://orcid.org/0000-0002-1699-6119
Andrew D King https://orcid.org/0000-0001-9006-5745
Todd P Lane https://orcid.org/0000-0003-0171-6927

References

Blamey R C, Ramos A M, Trigo R M, Tomé R and Reason C J C 2018 The influence of atmospheric rivers over the South Atlantic on winter rainfall in South Africa *J. Hydrometeorol.* **19** 127–42

Cordeira J M, Martin Ralph F and Moore B J 2013 The development and evolution of two atmospheric rivers in proximity to western north Pacific tropical cyclones in October 2010 *Mon. Weather Rev.* **141** 4234–55

Corringham T W, Martin Ralph F, Gershunov A, Cayan D R and Talbot C A 2019 Atmospheric rivers drive flood damages in the western United States *Sci. Adv.* **5** eaax4631

Cullen N J, Gibson P B, Mölg T, Conway J P, Sirguey P and Kingston D G 2019 The influence of weather systems in controlling mass balance in the Southern Alps of New Zealand *J. Geophys. Res.* **124** 4514–29

Dacre H F, Martínez-Alvarado O and Mbengue C O 2019 Linking atmospheric rivers and warm conveyor belt airflows *J. Hydrometeorol.* **20** 1183–96

Dean S, Rosier S, Carey-Smith T and Pa S 2013 The role of climate change in the two-day extreme rainfall in golden Bay, New Zealand, December 2011 *Bull. Am. Meteorol. Soc.* **94** S61–S63

DeFlorio M J *et al* 2019 Experimental subseasonal-to-seasonal (S2S) forecasting of atmospheric rivers over the Western United States *J. Geophys. Res.* **124** 11242–65

Eiras-Barca J, Lorenzo N, Taboada J, Robles A and Miguez-Macho G 2018 On the relationship between atmospheric rivers, weather types and floods in Galicia (NW Spain) *Nat. Hazards Earth Syst. Sci.* **18** 1633–45

Ericksen N and New Zealand National Water and Soil Conservation Authority 1986 Creating flood disasters?: New Zealand's need for a new approach to urban flood hazard (Wellington, New Zealand: Water and Soil Directorate, Ministry of Works and Development) **77**

Frame D J *et al* 2020 Climate change attribution and the economic costs of extreme weather events: a study on damages from extreme rainfall and drought *Clim. Change* **2020** 1–17

Gelaro R *et al* 2017 The modern-era retrospective analysis for research and applications, version 2 (MERRA-2) *J. Clim.* **30** 5419–54

Guan B and Waliser D E 2015 Detection of atmospheric rivers: evaluation and application of an algorithm for global studies *J. Geophys. Res.* **120** 12514–35

Hersbach H *et al* 2019 Global reanalysis: goodbye ERA-Interim, hello ERA5 *ECMWF Newsletter* **159** 17–24

ICNZ n.d. Cost of natural disasters | insurance council of NZ (ICNZ) (available at: www.icnz.org.nz/natural-disasters/cost-of-natural-disasters/) (Accessed 8 September 2020)

Kamae Y, Mei W, Xie S-P, Naoi M and Ueda H 2017 Atmospheric rivers over the Northwestern Pacific: climatology and interannual variability *J. Clim.* **30** 5605–19

Kidson J W 2000 An analysis of New Zealand synoptic types and their use in defining weather regimes *Int. J. Climatol.* **20** 299–316

Kingston D G, Lavers D A and Hannah D M 2016 Floods in the Southern Alps of New Zealand: the importance of atmospheric rivers *Hydrol. Process.* **30** 5063–70

Knapp K R *et al* 2011 Globally gridded satellite observations for climate studies *Bull. Am. Meteorol. Soc.* **92** 893–907

Lavers D A, Allan R P, Wood E F, Villarini G, Brayshaw D J and Wade A J 2011 Winter floods in Britain are connected to atmospheric rivers *Geophys. Res. Lett.* **38** n/a-n/a

Lavers D A, Pappenberger F and Zsoter E 2014 Extending medium-range predictability of extreme hydrological events in Europe *Nat. Commun.* **5** 781–797

Little K, Kingston D G, Cullen N J and Gibson P B 2019 The role of atmoshperic rivers for extreme ablation and snowfall events in the Southern Alps of New Zealand *Geophys. Res. Lett.* **46** 2761–71

Nayak M A and Villarini G 2017 A long-term perspective of the hydroclimatological impacts of atmospheric rivers over the central United States *Water Resour. Res.* **53** 1144–66

Newell R E, Newell N E, Zhu Y and Scott C 1992 Tropospheric rivers?—a pilot study *Geophys. Res. Lett.* **19** 2401–4

Paltan H, Waliser D, Lim W H, Guan B, Yamazaki D, Pant R and Dadson S 2017 Global floods and water availability driven by atmospheric Rivers *Geophys. Res. Lett.* **44** 10387–95

Pan M and Lu M 2020 East Asia atmospheric river catalog: annual cycle, transition mechanism, and precipitation *Geophys. Res. Lett.* **47** 1–10

Porhemmat R, Purdie H, Zawar-Reza P, Zammit C and Kerr T 2020 Moisture transport during large snowfall events in the New Zealand Southern Alps: the role of atmospheric rivers *J. Hydrometeorol.* **1** 425–44

Ralph F M, Neiman P J, Wick G A, Gutman S I, Dettinger M D, Cayan D R and White A B 2006 Flooding on California's Russian River: role of atmospheric rivers *Geophys. Res. Lett.* **33** 1–5

Ralph F *et al* 2019 A scale to characterize the strength and impacts of atmospheric rivers *Bull. Am. Meteorol. Soc.* **100** 269–89

Ramos A M, Trigo R M, Liberato M L R and Tomé R 2015 Daily precipitation extreme events in the Iberian Peninsula and its association with atmospheric rivers* *J. Hydrometeorol.* **16** 579–97

Reid K J, King A D, Lane T P and Short E 2020 The sensitivity of atmospheric river identification to integrated water vapor transport threshold, resolution, and regridding method *J. Geophys. Res.* **125** 1–15

Rosier S, Dean S, Stuart S, Carey-Smith T, Black M and Massey N 2015 Extreme rainfall in early July 2014 in Northland, New Zealand—was there and an anthropogenic influence? *Bull. Am. Meteorol. Soc.* **96** S136–S140

Rutz J J *et al* 2019 The atmospheric river tracking method intercomparison project (ARTMIP): quantifying uncertainties in atmospheric river climatology *J. Geophys. Res.* **124** 13777–802

Rutz J J, James Steenburgh W and Martin Ralph F 2015 The inland penetration of atmospheric rivers over western North America: a Lagrangian analysis *Mon. Weather Rev.* **143** 1924–44

Shields C A *et al* 2018 Atmospheric river tracking method intercomparison project (ARTMIP): project goals and experimental design *Geosci. Model Dev.* **11** 2455–74

Stidd C K 1953 Cube-root-normal precipitation distributions *Trans. Am. Geophys. Union* **34** 31

Tait A B and Fitzharris B B 1998 Relationships between New Zealand rainfall and south-west Pacific pressure patterns *Int. J. Climatol.* **18** 407–24

Valenzuela R A and Garreaud R D 2019 Extreme daily rainfall in central-Southern chile and its relationship with low-level horizontal water vapor fluxes *J. Hydrometeorol.* **20** 1829–50